ELSEVIER

Chemical Engineering Journal 132 (2007) 97–103

Chemical Engineering Journal

www.elsevier.com/locate/cej

Methane decomposition and self de-coking over gadolinia-doped ceria-supported Ni catalysts

Ta-Jen Huang *, Chun-Hsiu Wang

Department of Chemical Engineering, National Tsing Hua University, Hsinchu 300, Taiwan, ROC

Received 10 September 2006; received in revised form 21 December 2006; accepted 17 January 2007

Abstract

A temperature-programmed methane reaction with self de-coking and a fixed-temperature methane reaction were performed over gadolinia-doped ceria (GDC)-supported Ni catalysts. Experimental results reveal that, at below 810 °C, CO_2 formation rate is higher than that of CO, where below 700 °C, the latter is practically zero. The O species that is needed to form CO and CO_2 during and after CH_4 decomposition are supplied mainly from the bulk lattice of GDC. A drop in the supply rate of the O species from the GDC bulk lattice reduces the rates of CO and CO_2 formation; the CO formation rate decreases much more than the CO_2 formation rate. The CO and CO_2 formation rates can be controlled by both the mobility and the concentration of the bulk lattice oxygen. The concentration of the bulk lattice oxygen influences the self de-coking capability. Low temperature, low concentration of methane gas, or a short methane supply time can result in the formation of only CO_2 during self de-coking.

Keywords: Bulk lattice oxygen; Methane decomposition; Carbon monoxide; Carbon dioxide; Self de-coking; Gadolinia-doped ceria; Nickel catalyst

1. Introduction

For methane reactions, the nickel catalyst has been found to exhibit promising catalytic performance for steam reforming of methane [1,2] or carbon dioxide reforming of methane [3,4], both with methane decomposition as a reaction step. Methane decomposition over the nickel catalyst is well known to be associated with carbon deposition (coking) [5], which may lead to serious deactivation of the catalyst. However, the deposited carbon can be removed by gasification with steam [6] or carbon dioxide [7]. Recently, Huang et al. [8,9] demonstrated that, with doped ceria as the support, the nickel catalyst may have a self de-coking capability, i.e. the removal of the deposited carbon species via gasification by the O species supplemented from the lattice oxygen of the catalyst itself. In other words, "self de-coking" means de-coking in the absence of gaseous oxygen. Huang et al. [8] reported that only CO but no CO_2 was formed during CH_4 decomposition.

In a direct methane solid oxide fuel cell (SOFC) [10,11], CH_4 decomposition over the Ni cermet anode plays a critical role and the formation of only CO but not CO_2 should lead to a large difference in fuel efficiency for electricity generation. This is because the electrochemical formation of CO_2 involves four electrons while that of CO involves only two electrons, with each oxygen ion carrying two electrons; consequently, the current density associated with CO_2 formation is double that with CO formation. However, when the direct methane SOFC is adopted to carry out the cogeneration of syngas, the formation of only CO but not CO_2 is preferred. For SOFC with the deposited carbon (coke) as fuel [12], self de-coking is the only de-coking mechanism and CO or CO_2 formation is crucial on its performance of current generation. In either type of SOFC, the role of the bulk lattice oxygen in CO and CO_2 formations is important since the electrical current is produced with the transfer of oxygen species from the cathode to the anode via the bulk lattice of the oxides, i.e. the oxygen-ion conducting materials.

On the other hand, gadolinia-doped ceria (GDC) has been used as a support material of the nickel catalyst for methane decomposition and carbon gasification [8], for steam reforming of methane [9,13], and for carbon dioxide reforming of methane [9]. Additionally, GDC has been used as the anode cermet materials in direct methane SOFC [14]. However, a complete CO and CO_2 formation mechanism for methane decomposition over Ni catalysts supported on any of the oxygen-ion conducting materials has not yet been reported.

* Corresponding author. Tel.: +886 3 5716260; fax: +886 3 5715408.
E-mail address: tjhuang@che.nthu.edu.tw (T.-J. Huang).

1385-8947/$ – see front matter © 2007 Elsevier B.V. All rights reserved.
doi:10.1016/j.cej.2007.01.024

This work has derived the essential reaction steps in the CO and CO_2 formation mechanism for self de-coking during and after CH_4 decomposition over Ni supported on GDC, a member of the doped ceria family and of the oxygen-ion conducting materials. The role of the bulk lattice oxygen in CO and CO_2 formations is elucidated with these reaction steps and the associated analysis of CO and CO_2 formation rates.

2. Experimental

2.1. Preparation of gadolinia-doped ceria

Gadolinia-doped ceria (GDC) was prepared by co-precipitation. The details of the method have been reported elsewhere [8]. Appropriate amounts of gadolinium nitrate and cerium nitrate were used to make a nominal atomic ratio of Gd:Ce = 1:9. The GDC powders were calcined by heating in air at a rate of 10 °C/min to 300 °C and held for 2 h, and then at a rate of 10 °C/min to 700 °C and held for 4 h before slow cooling to room temperature. GDC prepared in this work is $(GdO_{1.5})_{0.1}(CeO_2)_{0.9}$. The BET surface area is 14.35 m^2/g.

2.2. Preparation of supported catalysts

The supported nickel catalyst was prepared by impregnating GDC powders with an appropriate amount of aqueous solution of nickel nitrate trihydrate, $Ni(NO_3)_2{\cdot}3H_2O$ (99.999% purity, SHOWA, Japan) for 7 h. After excess water was evaporated at 80 °C, the catalysts were dried in vacuum at 110 °C for 10 h. The catalysts were calcined by the same procedure as was used for the GDC powder. In this work, Ni catalysts are always supported over GDC and the indicated metal loading is a weight percentage with respect to the weight of the GDC support. The Ni loading is always 1 wt%, except noted otherwise.

2.3. Temperature-programmed reaction of methane

The tests of temperature-programmed reaction of methane (CH_4-TPRx) were conducted in a continuous flow reactor charged with 100 mg of sample catalyst, which was fixed by quartz wool and quartz sand downstream of the bed. The reactor was made of an 8 mm-ID quartz U-tube that was embedded in an insulated electric furnace. A K-type thermocouple was inserted into the catalyst bed to measure and control the bed temperature. The gas feed was passed through an oxygen filter to eliminate trace amounts of oxygen. A blank test was performed and the results indicated that no oxygen leak occurs in this reactor system.

The test was carried out with or without pre-reduction, as stated in the text. The catalyst was maintained in flowing argon until the designated test temperature was reached. A mixture of 1% CH_4 in argon was then fed to the catalyst bed at a flow rate of 20 ml/min and CH_4-TPRx started from room temperature to 880 °C at a rate of 10 °C/min and then held at 880 °C for 1 h before cooling. The reactor outflow was analyzed on-line by gas chromatograph (China Chromatograph 8900, Taiwan), CO-NDIR (Beckman 880), and CO_2-NDIR (Beckman 880).

2.4. Fixed-temperature reaction of methane

The fixed-temperature test was conducted in the same reactor setup as the CH_4-TPRx test, with 100 mg of sample catalyst. The catalyst was reduced in 100 ml/min of 30% H_2 for 1 h at 400 °C. The reactor was then purged with argon flow until no hydrogen could be detected in the reactor outflow. Afterwards, a mixture of 25% CH_4 in argon was fed to the catalyst bed at a flow rate of 100 ml/min to conduct methane decomposition, in order to deposit carbon species at the catalyst surface, at 400 °C for 40 min.

2.5. Temperature-programmed self de-coking

After the above fixed-temperature test, the catalyst was cooled in argon flow until room temperature and no methane was detected in the reactor outflow. Then, temperature-programmed self de-coking test was performed in 20 ml/min flowing argon, with the temperature increased from room temperature at a rate of 10 °C/min to the designated temperature, which was held for 1 h before cooling. Then, after cooling to room temperature, the total amount of the deposited carbon that remained on the tested catalyst was measured using a method described elsewhere [15].

3. Results

3.1. Temperature-programmed and fixed-temperature reaction of methane

Fig. 1 reveals that only CO_2 was formed at a temperature of lower than about 700 °C during the temperature-programmed reaction of methane (CH_4-TPRx). At over 700 °C, CO began to be formed and, at temperature of over around 810 °C, CO formation rate becomes exceeding that of CO_2. During CH_4-TPRx until cooling, the total amount of CO formation, with 2164 μmol/g catalyst, markedly exceeds that of CO_2 with

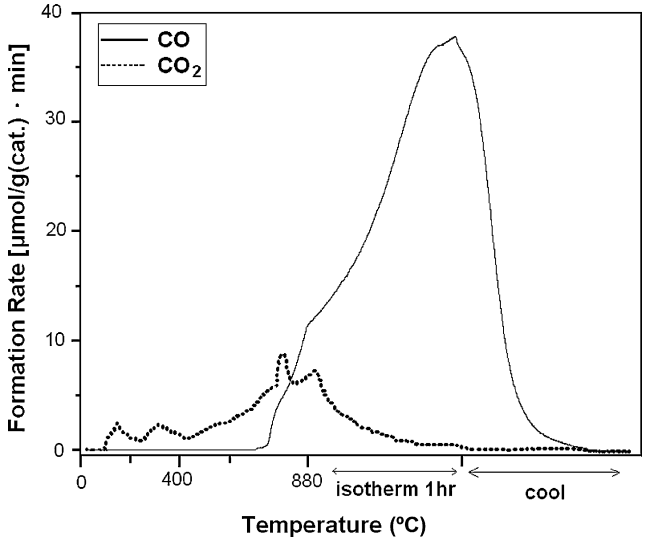

Fig. 1. Temperature-programmed reaction of methane over unreduced 0.3Ni/GDC.

Table 1
Average rates of CO and CO_2 formations during methane reaction at 400 °C for 40 min

	Average rate[a] (μmol/min g catalyst)	
	CO_2 formation	CO formation
GDC, 400 °C-reduced	26.4	1.4
Ni/GDC, 400 °C-reduced	28.5	21.7

[a] The average rate is calculated by dividing the integral reaction rate of 40 min by the reaction time (40 min).

387 μmol/g catalyst. Notably, the total O content of NiO in unreduced 0.3Ni/GDC is 51 μmol/g catalyst and that in GDC, i.e. $(GdO_{1.5})_{0.1}(CeO_2)_{0.9}$, is 11236 μmol/g catalyst. This clearly indicates that bulk lattice oxygen species of GDC are extensively involved in CO and CO_2 formations.

Table 1 indicates that methane activity, in terms of the total amount of CO and CO_2 formed, over Ni/GDC is much higher than that over pure GDC in the fixed-temperature reaction of methane at 400 °C. Over 400 °C-reduced Ni/GDC, the CO_2 formation at 400 °C exceeds that of CO. In Fig. 2, the CO formation rate at 400 °C becomes negligible over catalysts pre-reduced at 600 and 700 °C, unlike over those pre-reduced at 400 °C. On the other hand, although the CO_2 formation rate also declines as the pre-reduction temperature increases from 400 to 600 °C, still a considerable amount of CO_2 is formed, as shown in Fig. 3. However, the CO_2 formation rate increases instead as the pre-reduction temperature increases further to 700 °C. Furthermore, the CO_2 formation rates are higher or much higher than those of CO, with the latter possibly negligible; this is a same trend as that during CH_4-TPRx below 700 °C. Notably, the formations of di-hydrogen and water were confirmed via GC measurements.

3.2. Temperature-programmed self de-coking

Fig. 4 presents the self de-coking profiles of CO and CO_2 formations over Ni/GDC, over which carbon deposition (coking) was performed with 40 min methane flow. Notably, the CO peak at about 690 °C during self de-coking test is absent during CH_4-TPRx. Additionally, the temperature of this CO peak is approximately 100 °C higher than that of the lower-temperature CO_2 peak, at about 590 °C.

For a comparison, Fig. 5 shows that CO formation over GDC is relatively negligible below 800 °C and only a very small CO_2 peak is present at below 650 °C. In Fig. 6, with only 5 min methane flow over Ni/GDC, the CO_2 formation is almost complete, i.e. with a CO_2 selectivity of 100%.

The Ni/GDC catalysts in Figs. 4 and 6 were pre-reduced at 400 °C. Temperature-programmed self de-coking tests with pre-reduction at 600 and 700 °C were conducted to elucidate the effect of the pre-reduction temperature on the self de-coking capability of Ni/GDC. As shown in Table 2, pre-reduction at 600 °C only slightly reduces the self de-coking capability while pre-reduction at 700 °C markedly reduces it. Fig. 7 reveals that

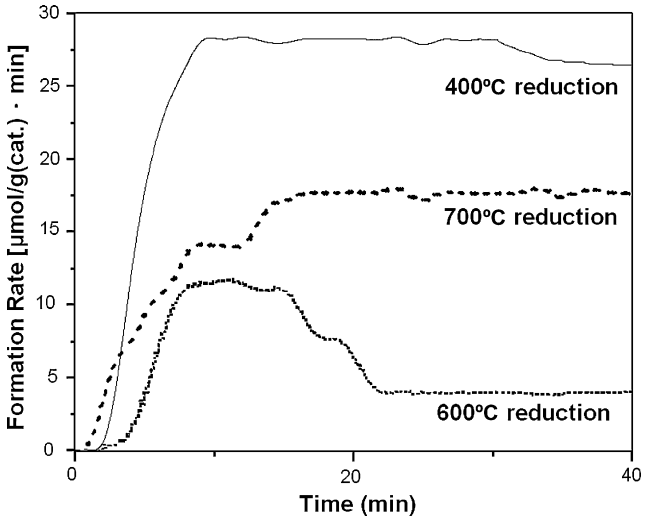

Fig. 3. CO_2 formation during methane decomposition at 400 °C over 1Ni/GDC pre-reduced at various temperatures.

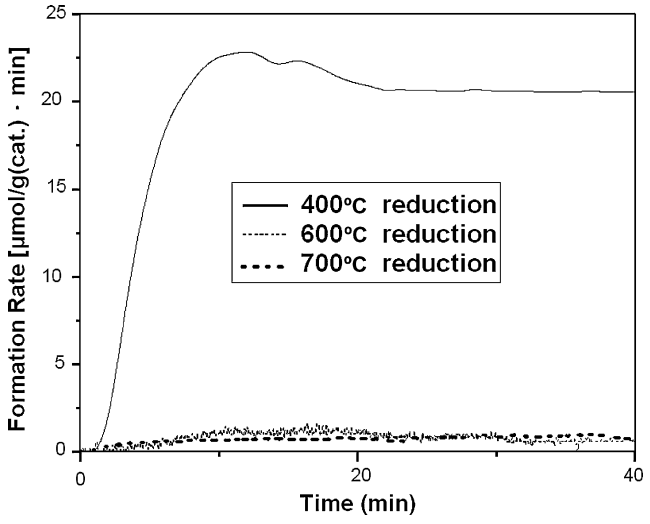

Fig. 2. CO formation during methane decomposition at 400 °C over 1Ni/GDC pre-reduced at various temperatures.

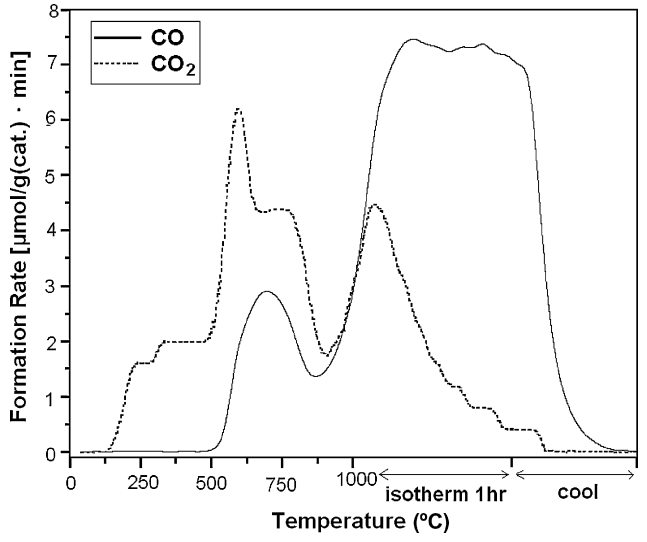

Fig. 4. Temperature-programmed self de-coking over 400 °C-reduced 1Ni/GDC after 40 min of methane decomposition.

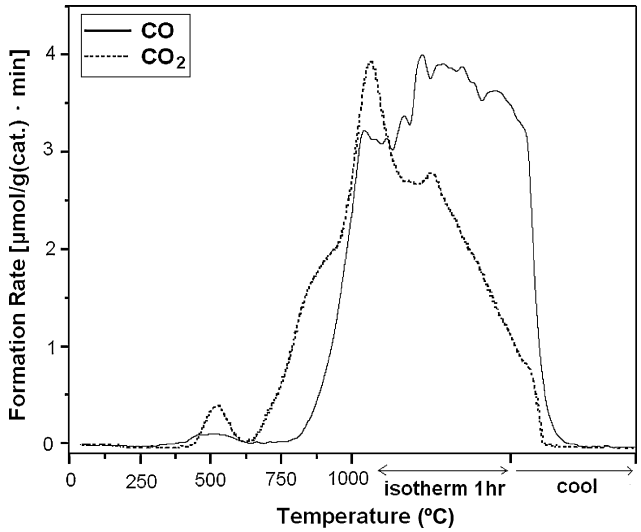

Fig. 5. Temperature-programmed self de-coking over 400 °C-reduced GDC after 40 min of methane decomposition.

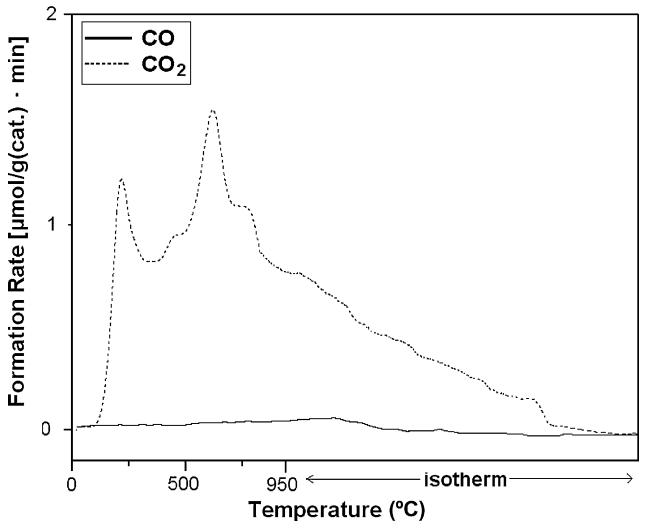

Fig. 6. Temperature-programmed self de-coking over 400 °C-reduced 1Ni/GDC after 5 min of methane decomposition.

Table 2
Amount of deposited carbon removed during temperature-programmed self de-coking[a] until cooled down to room temperature

	Pre-reduction temperature (°C)	Amount of deposited carbon ($\times 10^2$ μmol/g catalyst)		Self de-coking capability[b]
		Self de-coking	Remaining[c]	
GDC	400	4.8	7.6	0.38
Ni/GDC	400	8.7	8.8	0.50
Ni/GDC	600	5.6	5.9	0.49
Ni/GDC	700	1.5	16.4	0.08

[a] The time of methane flowing over the catalyst for carbon deposition was 40 min.

[b] Self de-coking capability = the ratio of the amount of deposited carbon removed during self de-coking to that of total deposited carbon, where the total deposited carbon is the sum of "self de-coking" plus "remaining".

[c] Denotes the amount of deposited carbon removed with 20 ml/min of 20% oxygen in argon at 900 °C after self de-coking.

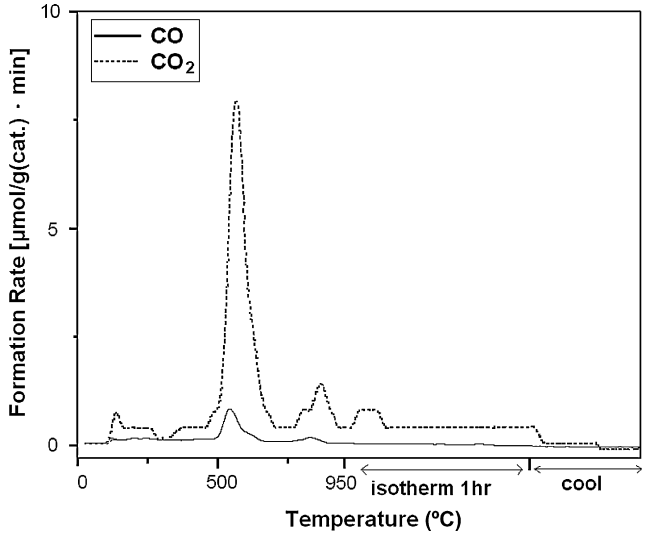

Fig. 7. Temperature-programmed self de-coking over 700 °C-reduced 1Ni/GDC after 40 min of methane decomposition.

pre-reduction at 700 °C markedly reduces the formation of CO_2 and almost totally eliminates that of CO; nevertheless, characteristic peaks similar to those of CO and CO_2 formations in the temperature range 500–700 °C remain for 400 °C-reduced Ni/GDC.

Table 3 shows that the CO_2 selectivity over 400 °C-reduced GDC exceeds that over 400 °C-reduced Ni/GDC, as in the fixed-temperature methane reaction at 400 °C, as can be figured out by the results in Table 1. When the pre-reduction temperature increases, the amounts of both CO and CO_2 formed during the self de-coking test over Ni/GDC drop; however, the amount of CO formation decreases much more than that of CO_2 and thus the CO_2 selectivity increases, as shown in Table 3.

On the other hand, Table 2 demonstrates that the total amounts of deposited carbon, i.e. the amount of self de-coked plus that remained, over 400 and 700 °C pre-reduced Ni/GDC are about the same, but that over 600 °C pre-reduced Ni/GDC is lower. The latter result is attributed to catalyst deactivation as evidenced by the drop of the CO_2 formation rate over 600 °C pre-reduced Ni/GDC, as shown in Fig. 3, which indicates a decrease in the CH_4 decomposition activity and thus a decrease of the total amount of deposited carbon.

4. Discussion

4.1. Role of bulk lattice oxygen in CO and CO_2 formations

The decomposition of CH_4 over Ni catalysts is usually considered as [1,8,16]:

$$CH_4 \rightarrow CH_x + (4-x)H \quad (1)$$

with $x = 0$–3. Notably, over Ni(1 1 1), the CH species has been identified as the surface species from CH_4 decomposition and is more stable than the CH_3 species [16]. The formed C species may accumulate to become coke and cause catalyst deactivation,

Table 3
Total amounts of CO and CO_2 formations during temperature-programmed self de-coking[a] until cooled down to room temperature

	Pre-reduction temperature (°C)	Total amount ($\times 10^2$ μmol/g catalyst)		CO_2 selectivity[b]
		CO_2 formation	CO formation	
GDC	400	2.4	2.3	0.51
Ni/GDC	400	3.7	5.1	0.42
Ni/GDC	600	3.4	2.2	0.60
Ni/GDC	700	1.4	0.1	0.93

[a] The time of methane flowing over the catalyst for carbon deposition was 40 min.
[b] CO_2 selectivity = CO_2 formation/(CO formation + CO_2 formation).

as evidenced by the decrease of the CO_2 formation rate shown in Fig. 3.

In the presence of the surface O species, the CH_x species can be oxidized to form CO and CO_2. However, the above results of CH_4-TPRx and self de-coking tests indicate that CO_2 was formed first, at a temperature that is lower than that of CO formation. Moreover, the fixed-temperature CH_4 reaction at 400 °C forms more CO_2 than CO. Thus, at low temperature, the following reactions to form CO_2 are considered to occur first (x = 1–3):

$$CH_x + O \rightleftarrows CHO + (x-1)H \quad (2)$$

$$CHO + O \rightarrow CO_2 + H \quad (3)$$

where O denotes an O species over Ni or in the surface oxygen vacancy of GDC at the Ni-GDC interface. Bitter et al. [17] proposed a mechanism of CO_2/CH_4 reforming over Pt-ZrO_2 catalyst, indicating that the CHO species is formed from the CH species which is produced by the dissociation of CH_4 over Pt metal and the surface O species from CO_2 over ZrO_2. This is reaction (2) with x = 1.

During self de-coking, the intermediate CHO species may be formed by the following reaction of the surface C species, which are the CH_x species with x = 0:

$$C + OH \rightleftarrows CHO \quad (4)$$

The OH species can be formed by subtracting H from methane or its decomposition intermediates using the O species [18]:

$$H + O \rightleftarrows OH \quad (5)$$

Notably, the combination of reactions (4) and (5) is reaction (2) with x = 1 if the dissociation of the CH species is regarded as CH → C + H [16]. Then, CO_2 is formed via reaction (3).

The O species in the above reactions may be the lattice oxygen species that is initially present over surface, such as those in NiO, or may be supplemented from the bulk lattice oxygen of GDC, which results in "self de-coking". Notably, the O species in the surface oxygen vacancy may be removed and refilled due to the mobility of oxygen. Before CO is formed during CH_4-TPRx, at about 700 °C as shown in Fig. 1, the amount of CO_2 formation is 141 μmol/g catalyst, equivalent to the consumption of 282 μmol/g catalyst of O species, which is much higher than the total O content of 51 μmol/g catalyst in NiO of the unreduced 0.3Ni/GDC catalyst. Notably, NiO can be reduced to Ni at 400 °C [19]. This indicates that most of the O species for CO_2 formation is from the bulk lattice oxygen of GDC. Notably, also, the O species may migrate via surface diffusion from the Ni-doped ceria interface to the Ni surface [19].

With possible CHO species as an intermediate for CO_2 formation, CO may be formed by the dissociation of CHO [20]:

$$CHO \rightarrow CO + H \quad (6)$$

Reaction (3) is the oxidative dehydrogenation of the CHO species and may be preferred over CHO dissociation, reaction (6). This agrees with the results of Table 1, which reveal that CO_2 formation rate is higher than that of CO. Furthermore, as shown in Fig. 4, the CO_2 peak at about 590 °C is at a temperature that is 100 °C lower than the CO peak at about 690 °C. Therefore, it can be concluded that the rate of reaction (3) to form CO_2 is higher than that of reaction (6) to form CO.

As stated above, at a temperature of lower than 700 °C, the partial oxidation of the CH_x species to CO directly rather than to the intermediate CHO species is less likely since CO_2 is formed before CO via the CHO intermediate. The formation of the intermediate CHO species, by reaction (2) or (4), followed by its oxidation and dissociation to produce CO_2 and CO, respectively, seems to be the most probable explanation of the 100 °C difference between CO_2 and CO peaks in the temperature range 500–700 °C.

Reaction steps (3) and (6) above are essential to the formation of CO_2 and CO, especially at low temperature. Nevertheless, these reactions may occur also at high temperature to remove CH_x, the coke precursor. Therefore, the removal of CH_x by its oxidation with the O species from the bulk lattice is expected to reduce or even stop coke formation. Consequently, coking and the resulting catalyst deactivation can be prevented.

At a temperature of higher than about 810 °C, the CO formation rate becomes higher than that of CO_2, as shown in Fig. 1. This may be attributed to higher CHO dissociation rate, reaction (6), due to higher temperature. However, since the rate of CO formation can greatly markedly exceed that of CO_2, other reactions to form CO but not CO_2 should have occurred, such as the partial oxidation of the CH_x species. However, the results presented in Fig. 6 exclude the possibility of the gasification of the surface C species by the formed CO_2 species, $C + CO_2 \rightarrow 2CO$.

4.2. Analysis of CO and CO_2 formation rates

As discussed above, at temperature of below 700 °C, the rate of oxidation of CHO to CO_2 exceeds the rate of its dissociation to CO. Thus, the almost complete CO_2 formation, shown in

Fig. 6, can be attributed to the complete oxidation of the CHO species, rather than its dissociation, by the relatively abundant O species, since the concentration of the deposited carbon species to consume the O species in CHO formation beforehand is relatively low. Notably, the very short period of methane flow is responsible for the very low concentration of the deposited carbon species, as shown in Fig. 6. Then, increasing the rate of the CHO reaction to form CO_2 rather than CO leads to the almost complete CO_2 formation. Notably, the low concentration of the deposited carbon species results in the low CHO concentration; this reduces the formation rate of CO since it is lower than that of CO_2, as also shown in Fig. 7. Hence, it can be concluded that a low concentration of deposited carbon species can lead to the formation of only CO_2 during self de-coking. Notably, a low concentration of the deposited carbon species can be obtained using a low concentration of CH_4 gas, a short CH_4 supply time, or low temperature, all of which lead to low CH_4 conversion.

At low temperature, the mobility of the lattice oxygen is low and the O species for CO and CO_2 formations may not be able to be fully supplied if the concentration of the deposited carbon species is high. Therefore, the rate of carbon removal may not be sufficiently high and coking occurs to deactivate the catalyst, as in 600 °C pre-reduced Ni/GDC, shown in Fig. 3. Notably, the 600 °C pre-reduction removes not only all of the surface lattice oxygen but also some of the bulk lattice oxygen near the surface [18]; hence, the supply rate of the O species for carbon removal markedly decreases. Notably, also, the supply rate of the O species from the bulk lattice depends on both the oxygen mobility and the concentration of the bulk lattice oxygen.

As the pre-reduction temperature increases to 700 °C, which is close to the temperature at which the lattice oxygen to be highly mobile [21], the bulk lattice oxygen can be redistributed close to the surface at a sufficiently high rate [22]. Consequently, the supply rate of the O species for CO and CO_2 formations can be restored to a particular level to reduce or even prevent catalyst deactivation associated with coking. This explains why the 700 °C pre-reduced Ni/GDC outperforms the 600 °C pre-reduced Ni/GDC, as displayed in Fig. 3.

As the pre-reduction temperature increases, the concentration of bulk lattice oxygen should drop because of the increased reduction. Thus, the supply rate of the O species declines and both CO and CO_2 formation rates should fall. This is in agreement with the results that are presented in Table 3. Therefore, it can be concluded that the concentration of the bulk lattice oxygen affects the rates of CO and CO_2 formations. Furthermore, the decrease of CO and CO_2 formations during self de-coking test means a drop of the self de-coking capability, as shown in Table 2. Therefore, it can also be concluded that the concentration of the bulk lattice oxygen affects the self de-coking capability.

Comparing Figs. 1 and 2 reveals the effect of the concentration of CH_4 in the gas phase. As shown in Fig. 2, CH_4 decomposition at 400 °C can result in the formation of a relatively large amount of CO, in comparison to zero CO formation at 400 °C during CH_4-TPRx, in Fig. 1. Given that the temperature is the same, the major difference between Figs. 1 and 2 is in the concentration of gaseous CH_4. With CH_4-TPRx, the gaseous CH_4 concentration is 1%, which is relatively low for revealing the peak characteristics, while that for fixed-temperature CH_4 decomposition is 25%, which is relatively high for accelerating carbon deposition. This verifies that a low concentration of CH_4 gas can result in the formation of CO_2 only.

For direct methane SOFC, the above rate analysis indicates that intermediate-temperature SOFC (IT-SOFC) with an operating temperature of below 700 °C can achieve complete CO_2 formation, and thus high fuel efficiency in generating electricity. On the other hand, high temperature SOFC, with an operating temperature of over 900 °C, can produce mostly CO and is more effective in the cogeneration of electricity and syngas than is IT-SOFC.

5. Conclusions

1. For reaction temperatures at below 810 °C, CO_2 formation rate is higher than that of CO, where below 700 °C, the latter is practically zero.
2. The O species that is needed to form CO and CO_2 for self de-coking during and after CH_4 decomposition are supplied mainly from the bulk lattice of GDC.
3. A drop in the supply rate of the O species from the GDC bulk lattice reduces the rates of CO and CO_2 formation; the CO formation rate decreases much more than the CO_2 formation rate.
4. The CO and CO_2 formation rates can be controlled by both the mobility and the concentration of the bulk lattice oxygen.
5. The concentration of the bulk lattice oxygen influences the self de-coking capability.
6. Low temperature, low concentration of methane gas, or a short methane supply time can result in the formation of only CO_2 during self de-coking.

References

[1] Y. Matsumura, T. Nakamori, Steam reforming of methane over nickel catalysts at low reaction temperature, Appl. Catal. A: Gen. 258 (2004) 107–114.
[2] S. Rakass, H. Oudghiri-Hassani, P. Rowntree, N. Abatzoglou, Steam reforming of methane over unsupported nickel catalysts, J. Power Sources 158 (2006) 485–496.
[3] J.R. Rostrup-Nielsen, J.H. Bak Hansen, CO_2-reforming of methane over transition metals, J. Catal. 144 (1993) 38–49.
[4] Z. Hao, H.Y. Zhu, G.Q. Lu, Zr-laponite pillared clay-based nickel catalysts for methane reforming with carbon dioxide, Appl. Catal. A: Gen. 242 (2003) 275–286.
[5] M.A. Ermakova, D.Y. Ermakov, G.G. Kuvshinov, L.M. Plyasova, New nickel catalysts for the formation of filamentous carbon in the reaction of methane decomposition, J. Catal. 187 (1999) 77–84.
[6] V.R. Choudhary, S. Banerjee, A.M. Rajput, Hydrogen from step-wise steam reforming of methane over Ni/ZrO_2: factors affecting catalytic methane decomposition and gasification by steam of carbon formed on the catalyst, Appl. Catal. A: Gen. 234 (2002) 259–270.
[7] J.B. Wang, Y.S. Wu, T.J. Huang, Effects of carbon deposition and de-coking treatments on the activation of CH_4 and CO_2 in CO_2 reforming of CH_4 over Ni/yttria-doped ceria catalysts, Appl. Catal. A: Gen. 272 (2004) 289–298.
[8] T.J. Huang, T.C. Yu, Effect of steam and carbon dioxide pretreatments on methane decomposition and carbon gasification over doped-ceria supported nickel catalyst, Catal. Lett. 102 (2005) 175–181.

[9] T.J. Huang, H.C. Lin, T.C. Yu, A comparison of oxygen-vacancy effect on activity behaviors of carbon dioxide and steam reforming of methane over supported nickel catalysts, Catal. Lett. 105 (2005) 239–247.
[10] J.B. Wang, J.C. Jang, T.J. Huang, Study of Ni-samaria-doped ceria anode for direct oxidation of methane in solid oxide fuel cells, J. Power Sources 122 (2003) 122–131.
[11] Y. Lin, Z. Zhan, J. Liu, S.A. Barnett, Direct operation of solid oxide fuel cells with methane fuel, Solid State Ionics 176 (2005) 1827–1835.
[12] M. Ihara, K. Matsuda, H. Sato, C. Yokoyama, Solid state fuel storage and utilization through reversible carbon deposition on an SOFC anode, Solid State Ionics 175 (2004) 51–54.
[13] T.J. Huang, T.C. Yu, S.Y. Jhao, Weighting variation of water-gas shift in steam reforming of methane over supported Ni and Ni–Cu catalysts, Ind. Eng. Chem. Res. 45 (2006) 150–156.
[14] A.A. Yaremchenko, A.A. Valente, V.V. Kharton, I.A. Bashmakov, J. Rocha, F.M.B. Marques, Direct oxidation of dry methane on nanocrystalline $Ce_{0.8}Gd_{0.2}O_{2-\delta}$/Pt anodes, Catal. Commun. 4 (2003) 477–483.
[15] T.J. Huang, S.Y. Jhao, Ni-Cu/samaria-doped ceria for catalytic steam reforming of methane in the presence of carbon dioxide, Appl. Catal. A: Gen. 302 (2006) 325–332.
[16] Q.Y. Yang, K.J. Maynard, A.D. Johnson, S.T. Ceyer, The structure and chemistry of CH_3 and CH radicals adsorbed on Ni(1 1 1), J. Chem. Phys. 102 (1995) 7734–7749.
[17] J.H. Bitter, K. Seshan, J.A. Lercher, Mono and bifunctional pathways of CO_2/CH_4 reforming over Pt and Rh based catalysts, J. Catal. 176 (1998) 93–101.
[18] J.H. Jun, T.H. Lim, S.W. Nam, S.A. Hong, K.J. Yoon, Mechanism of partial oxidation of methane over a nickel–calcium hydroxyapatite catalyst, Appl. Catal. A: Gen. 312 (2006) 27–34.
[19] J.B. Wang, S.Z. Hsiao, T.J. Huang, Study of carbon dioxide reforming of methane over Ni/yttria-doped ceria and effect of thermal treatments of support on the activity behaviors, Appl. Catal. A: Gen. 246 (2003) 197–211.
[20] E. Heracleous, A.A. Lemonidou, Homogeneous and heterogeneous pathways of ethane oxidative and non-oxidative dehydrogenation studied by temperature-programmed reaction, Appl. Catal. A: Gen. 269 (2004) 123–135.
[21] C.H. Wang, Study of Self Decoking over Gadolinia-doped Ceria Supported Ni and Fe Catalysts after Methane Reaction, Master Thesis, National Tsing Hua University, Taiwan, 2006.
[22] T.J. Huang, M.C. Huang, A new phenomenon of a fuel-free current during intermittent fuel flow over Ni-YSZ anode for direct methane SOFCs, J. Power Sources, submitted for publication.